RSC Advances

ROYAL SOCIETY OF CHEMISTRY

www.rsc.org/advances

RSC Advance

RSCPublishing

ARTICLE

An electrochemical strategy with molecular beacon and hemin/G-quadruplex for the detection of *Clostridium perfringens* DNA on screen-printed electrodes

Cite this: DOI: 10.1039/x0xx00000x

Received 00th January 2014,
Accepted 00th January 2014

DOI: 10.1039/x0xx00000x

www.rsc.org/

Dongneng Jiang, Fei Liu, Liqun Zhang, Linlin Liu, Chang Liu, and Xiaoyun Pu*

C. perfringens is a prevalent pathogen that causes infectious disease. It becomes viable easily but often cannot be cultured and thus escapes detection. Here, we describe an electrochemical strategy based on molecular beacon (MB), streptavidin (SA), and hemin/G-quadruplex/Fe_3O_4 nanocomposites. Initially, the MB forms a stable hairpin, which blocks the binding capability of the SA aptamer. After incubating with target DNA, the hairpin opens and the SA aptamer is reactivated to capture the SA/alcohol dehydrogenase(ADH)/Fe_3O_4 nanocomposites. Through a "sandwich" reaction, the hemin/G-quadruplex is captured on the electrode surface, and the electrochemical signal of DPV is thus obtained. Our results suggest that the use of AuNPs/graphene dramatically enlarges the surface area and enhances the immobilisation of the capture probe (MB). The combination of the Fe_3O_4 nanocomposite with hemin/G-quadruplex enabled the progressive amplification of electrochemical signal. It also showed satisfying stability, reproducibility and good specificity. Compared with PCR, there were no significant differences in the recovery and regression of concentration. Thus, this SPE strategy is a promising alternative for detecting *C. perfringens* without bacterial culture and DNA amplification in point of care testing (POCT).

Introduction

C. perfringens is an anaerobic bacillus that is associated with malignant diseases and near-term pregnancies.[1] People are at risk of autoinfection if they are wounded by trauma or major surgery and do not receive adequate treatment.[2] The necrotic tissue processes fuels the proliferation of *C. perfringens*, leading to gas gangrene and, subsequently, sepsis.[3] *C. perfringens* uses chromosomally encoded alpha toxin and perfringolysin O during histotoxic infections. Therefore, the detection of *C. perfringens* is highly important in clinical diagnosis. [4, 5] Traditional methods are primarily based on bacteriological culture,[6] which are considered the "gold standard" but generally suffer from the disadvantages of being time consuming and tedious.[7] Previously, methods to identify *C. perfringens* by PCR assays have been reported.[4] Other methods have received particular attention, including microarray [8] and immunochromatographic assay.[9] However, these methods generally require highly precise thermal equipment and suffer from the loss of amplification specificity.[10] Thus, it is very important to develop new techniques to rapidly and sensitively detect *C. perfringens*.

Electrochemical sensors have played an important role in the detection of DNA, RNA, protein and trace elements because of their advantages, such as simple instrumentation, fast response, high specificity and sensitivity.[11] Moreover, multiple nanomaterials have emerged for use in fabricating signal-amplified biosensors. Among them, graphene is widely used and has the advantages of flexibility, a large surface area, and excellent electrical conductivity.[12] Thus, it was employed as an enzyme immobilised platform in this work. Hemin is the active centre of haemoglobin and can generate electrochemical signals.[13] Additionally, it possesses excellent peroxidase activity as well as good stability and ease of self-replication.[14] An electrochemical aptasensor based on hemin/G-quadruplex and Fe_3O_4-Au nanocomposites was previously reported.[15] Both the Fe_3O_4-Au nanocomposites and hemin/G-quadruplex could catalyse the reduction of the generated H_2O_2, which promoted the electronic transfer and amplified the electrochemical signal. Recently, screen printed electrodes (SPE) have been widely applied in electrochemical analysis because of their various advantages, including low cost, minimal time requirements and miniaturisation.[16] An electrochemical aptasensor involving silica nanospheres coated with quantum dots and SPE has also been reported.[17] Additionally, a multi-channel electrode array sensing device fabricated by SPE using a 96-well plate as the template has been described.[18] Further, a label-free direct electrochemical immunosensor for detecting cytochrome c based on polypyrrole (PPy) grafted SPE has been reported.[19] Therefore, this study utilises a reliable technical basis of graphene, hemin/G-quadruplex, Fe_3O_4 nanocomposites, and SPE.

*Department of clinical laboratory, Xinqiao Hospital, Third military medical university, Chongqing 400037, P. R. China. *Corresponding author. E-mail: xqyyjyk@foxmail.com. Fax/Tel: +86-023-68755637*

Here, we describe an electrochemical strategy aptasensor based on molecular beacon (MB),[20] hemin/G-quadruplex [21] and alcohol dehydrogenase (ADH) [22] labelled Fe_3O_4 nanocomposites.[23] First, the MB labelled graphene-GCE and ADH/hemin/G-quadruplex/Fe_3O_4 nanocomposite were prepared. In this manner, more MB could be immobilised on the nanocomposite sheet due to the increased large surface area. The MB formed a hairpin and blocked the binding of SA. After incubation with target DNA, the hairpin opened and the streptavidin (SA) aptamer region could capture the SA-ADH/hemin/G-quadruplex/Fe_3O_4 nanocomposite. According to previous reports, the hemin/G-quadruplex acts not only as a horseradish peroxidase mimicking DNAzyme but also as an NADH oxidase and NADH peroxidase mimicking DNAzyme. Therefore, in the presence of H_2O_2 and NADH, the hemin/G-quadruplex and ADH effectively catalysed the conversion of alcohol to acetaldehyde.[24] The electrochemical signal could be measured by Differential Pulse Voltammetry (DPV).[25] Finally, the SPE was assembled for the detection of *C. perfringens*. The strategy of this work is shown in **Scheme 1**.

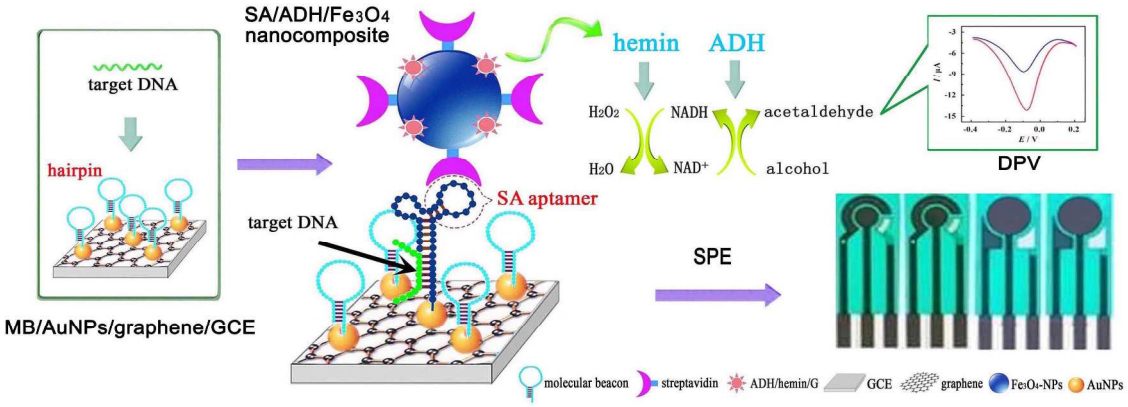

Scheme 1. The principle of the electrochemical aptasensor.

Experimental Methods

Chemicals and materials

SA, hemin, hexanethiol (HT), bovine serum albumin (BSA), $HAuCl_4$, alcohol dehydrogenase (ADH), β-nicotinamide adenine dinucleotide hydrate (NADH), and Poly (diallyl dimethyl ammonium chloride) (PDDA) were obtained from Sigma-Aldrich (St. Louis., MO, USA). Graphene was purchased from Xianfeng (Nanjing, China) and Fe_3O_4 magnetic microspheres from Nachen (Beijing, China). DNA pure kits were gained from Tiangen (Beijing, China). The ultrapure water was prepared by Milli-Q (Millipore, USA).

Apparatus and electrode

Cyclic voltammetry (CV) and differential pulse voltammetry (DPV) were performed with a CHI 650D electrochemical work station (Shanghai, China) on the modified glassy carbon electrode (GCE, Φ= 4 mm) and SPE (Φ= 4 mm).

Preparation of AuNPs/graphene

First, 50 mL graphene (1 $g.L^{-1}$) and 0.5 mL hydrazine hydrate (80%) were mixed and stirred at 90°C for 12 h. The product was washed 5 times with ultrapure water. Then, the gold were electrodeposited on the graphene modified electrode surface at a constant potential of –0.2 V for 30 s. Finally, the morphology of AuNPs/graphene was studied by scanning electron microscope (SEM) S-4800 (Hitachi, Japan) and energy dispersive x-ray spectroscopy (EDX) EDX-720 (Shimadzu, Japan).

Fabrication process of the bisensor

The alpha toxin gene (Genbank: AB794298.1) was chosen as the target gene as it has been previously applied in PCR,[26] ELISA,[27] and bisensor studies.[2] The MB was designed by Beacon Designer 4.01 (Premier Biosoft, USA) and synthesised by Sangong (Shanghai, China). The synthetic target DNA contained the complementary fragment of MB, 5' end (6 bases), and 3' end (6 bases), to mimic the DNA of *C. perfringens* in samples. All sequences had been checked by BLAST of National Center for Biotechnology Information (NCBI, USA), and met the specific requirement of the biosensor. Sequence of MB: 5'-SH-$(CH_2)_3$-TTT TTTTTTTTGGCGTTCTTATGTTATCCACAACGCAGTGTGC GACATAAG-3'. Synthesised target DNA: 5'-GATATGATAAGA ACGCCTATGA-3'. The design of MB is shown in **Scheme 2**.

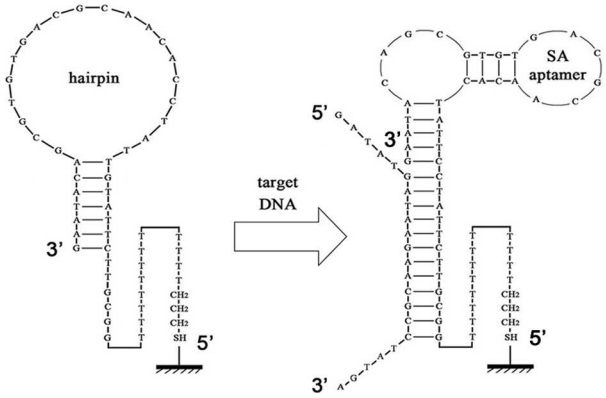

Scheme 2. The construction of molecular beacon.

First, the GCE was polished with 0.3 and 0.05 μm alumina powder separately, sonicated and rinsed with ultrapure water. Then, 50 μL graphene (hydrazine hydrate mixed) was dropped onto it and dried at room temperature. After that, gold was electrodeposited on the graphene/GCE at –0.2 V for 30 s. Next, 100 μL MB (0.5 mM) was heated to 90 °C for 5 min, 4 °C for 1 h, incubated with TCEP for 1 h, and coated onto the surface of AuNPs/graphene/GCE for 1 h. Finally, the aptasensor was treated with 100 μL HT (1 mM) to block the residual gold active sites. Electrochemical impedance

spectroscopy (EIS) was measured after every processing step to check the effect of the preparation. This was carried out in 5 mM $[Fe(CN)_6]^{3-/4-}$ with 0.1 M KCl, 5 mV, and the frequency ranging from 10 kHz to 50 MHz.

Preparation of SA-ADH-Fe_3O_4 nanocomposites

First, hemin/G-quadruplex labelled ADH (2 $g.L^{-1}$) was synthesised with EDC (2 $g.L^{-1}$). Then, 0.5 mL PDDA-protected Fe_3O_4 magnetic microspheres (50 mg/mL) was mixed with 0.5 mL ADH and SA (5 $g.L^{-1}$) in PBS (pH 7.4), sonicated for 10 min and stirred for 12 h at 4 °C. In addition, 0.1 mL BSA (1%) was added into the solution and stirred for 40 min to block the remaining active sites. The mixture was centrifuged at 12,000 rpm for 10 min and washed with ultrapure water to remove the unbounded ADH and SA. The morphology of SA/ADH/Fe_3O_4 nanocomposites was studied by transmission electron microscope (TEM) TECNAI 10 (Philips, Netherlands) and EDX-720. Then, it was centrifuged and separated magnetically. Finally, the detection of target DNA (10^{-6} M) was performed to evaluate the effect of the SA/ADH/Fe_3O_4 nanocomposites. The control group was prepared in the same manner as the detection group (SA/ADH/Fe_3O_4 nanocomposite), but the 0.5 mL Fe_3O_4 nanocomposite was replaced by 0.5 mL PBS (pH 7.4).

Construction of SPE aptasensor

The SPE was constructed by Changshanjiao (Shuzhou, China). Every SPE has 16 copies of three-electrodes. The electrodes were manufactured by squeezing a mixture containing carbon ink (for working and auxiliary electrode) and Ag-AgCl ink (for reference electrode) onto a polyethylene terephtalate support. After printing, the SPE was cured at 60 °C for 20 min. Next, the SPE was delimited using a tape for galvanoplasty. [28] Then, 50 µL graphene (hydrazine hydrate mixed) was dropped onto it and dried at room temperature. After that, gold was electrodeposited on the SPE at –0.2 V for 30 s. Then, 100 µL MB (0.5 mM) was heated to 90 °C for 5 min, 4 °C for 1 h, incubated with TCEP for 1 h, and coated onto the surface of AuNPs/SPE for 1 h. Finally, 100 µL HT (1 mM) was added to block the residual gold active sites. The reproducibility of the proposed SPE aptasensor was evaluated by determining 10^{-6} M target DNA using 10 prepared SPE aptasensors in the same conditions and the same electrode for 10 measurements. The relative standard deviation (RSD) of DPV was then calculated.

DNA detection of *C. perfringens*

A solution of synthesised target DNA was serially diluted (10^{-14}～10^{-4} M) and measured in the presence of 80 µL NADH (0.25 mM), 80 µL absolute ethanol, and 1 mL PBS (pH 7.4), with SA-ADH-Fe_3O_4 nanocomposites by DPV (4 mV potential incremental, 50 mV amplitude, 50 s pulse width, 0.0167 s sample width, 100 $mV.s^{-1}$ scan rate, and the potential range from -0.6 to 0.1 V). DNA of real bacteria was extracted from *C. perfringens* (ATCC 35150), which was obtained from American Type Culture Collection (ATCC, USA). The DNAs were extracted using the DNA pure kit. The concentration of the extracted DNA was estimated by DPV with SPE, adjusted to 10^{-4} M, and stored at -20 °C prior to use.

Comparison with PCR

ABI 7500 real-time PCR (ABI, USA) was used for PCR amplification. Primer 1: 5′-ATATGTCCAAAAGTGAACCAGAA AG-3′. Primer 2: 5'-TATCTGTATCAGGATCCCAGAAATG-3′. Probe: 5′-FAM-TATGATAAGAACGCCTAT-MGB/NFQ-3′. All sequences were designed by Primer Premier 5.0 (Premier Biosoft, Canada) and synthesised by Sangong (Shanghai, China) The DNAs of *C. perfringens* were denatured at 95°C for 5 min, followed by 40 cycles of 94°C for 30 s, 54°C for 45 s, 72°C for 30 s, and a final 3-min extension. The PCR products were resolved using 2% agarose gel electrophoresis and visualised by Gel logic 212 Imaging system (Kodak, USA). The same DNAs were detected by the aptasensor in the same time. Finally, the recovery rate and correlation of SPE aptasensor and PCR were analysed.

Results and discussion

Characterisations of AuNPs/graphene and SA/ADH/Fe_3O_4 nanocomposites

The morphology of AuNPs/graphene was analysed by SEM. As shown in Fig. 1A, graphene had a large lamellate and scrolled sheet, which provided a large surface area. After electrodeposition, a significant amount of Au-NPs was observed on the graphene (Fig. 1B). Furthermore, the EDX presented the significant signal of Au (Au1, 2, and 3) for the

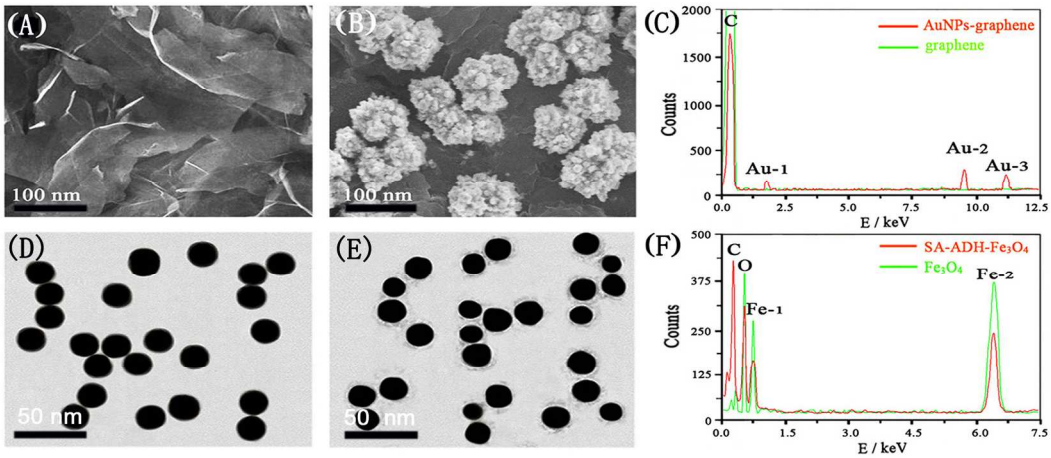

Fig. 1 Characterisations of AuNPs/graphene and SA/ADH/Fe_3O_4 nanocomposite. (A) SEM image of graphene; (B) SEM image of AuNPs/graphene; (C) EDX of AuNPs/graphene; (D) TEM image of Fe_3O_4 nanoparticles; (E) TEM image of SA/ADH/Fe_3O_4 nanocomposite; (F) EDX of SA/ADH/Fe_3O_4 nanocomposite.

resulting metallic, which further suggested the successful synthesis of AuNPs (Fig. 1C). TEM and EDX were employed to evaluate the synthesis of the SA/ADH/Fe_3O_4 nanocomposites. As shown in Fig. 1D, a significant number of Fe_3O_4 nanoparticles were observed. After being connected to ADH and SA, many filaments were observed around the Fe_3O_4 nanoparticles (Fig. 1E). In addition, the EDX presented a high signal of C, suggesting that there were more organic compounds in the nanocomposites, and low signals of O and Fe (Fe1, 2), indicating that the Fe_3O_4 nano-particles been partially covered (Fig. 1F). In short, the construction of SA/ADH/Fe_3O_4 nanocomposites was successful.

Characterisations of the stepwise modified aptasensor

To characterise the modified process of the aptasensor, EIS was performed (Fig. 2). First, the bare GCE showed a redox peak (curve a). After being coated with graphene, there was a slight change in impedance because of the similar composition of carbon (curve b). Following the electrodeposition of gold, the peak current increased significantly due to the superior conductivity of the AuNPs (curve c). The peak current was dramatically decreased after the incubation of MB on the electrode surface (curve d). After blocking with HT, a decrease in peak current was also observed (curve e). The resistance further increased when the electrode was incubated with target DNA (10^{-6} M, curve f), which was attributed to the complementary pairing of the SA aptamer and SA that retarded the electron transfer tunnel. These results suggested that the construction of the aptasensor was successful.

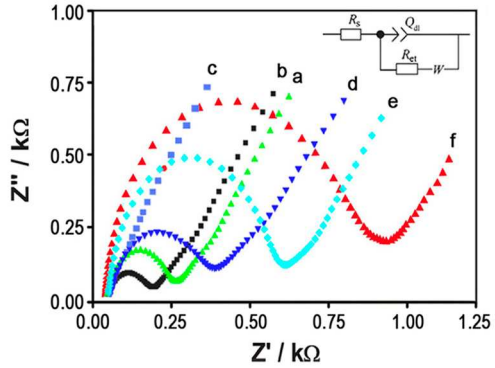

Fig. 2. EIS of the stepwise modified aptasensor. a) bare GCE; b) graphene/GCE; c) AuNPs/graphene/GCE; d) MB/AuNPs/graphene/GCE; e) HT/MB/AuNPs/graphene/GCE; f) target DNA/HT/MB/AuNPs/graphene/GCE.

Characterisations of the SA/ADH/Fe_3O_4 nanocomposite

The SA/ADH/Fe_3O_4 nanocomposite is shown in Fig. 3A. It could be uniformly distributed in the water after ultrasonic hydration or quickly separated by centrifugal or magnetic separation. There was no significant difference between centrifugal precipitation and magnetic separation. Therefore, it has the advantage of easy separation. Subsequently, the effect of detection was compared between SA/ADH (without Fe_3O_4 nanocomposites) and SA/ADH/Fe_3O_4 nanocomposites (Fig. 3B). The peak current (DPV) of SA/ADH/Fe_3O_4 nanocomposites was approximately 2 higher times than that without Fe_3O_4 nanocomposites. This result suggested that the large surface area of the Fe_3O_4 nanocomposites could support more ADH/hemin/G-quadruplexes, which led to a stronger signal.

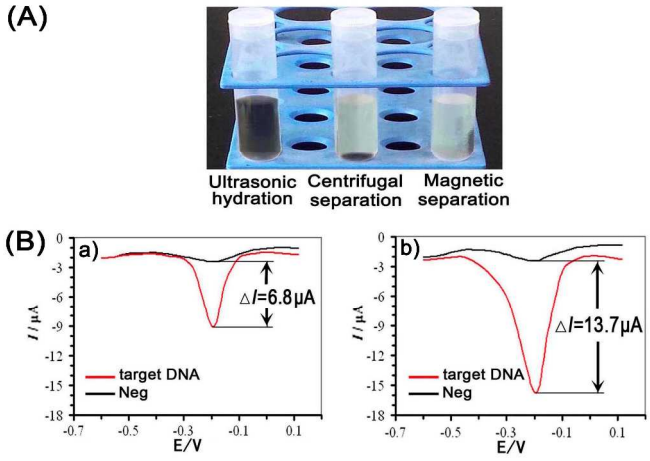

Fig. 3. Characterisations of the SA/ADH/Fe_3O_4 nanocomposite.(A) SA/ADH/Fe_3O_4 nanocomposite's centrifugal and magnetic separation; (B) DPV evaluation of Fe_3O_4 nanocomposite. a) SA/ADH without Fe_3O_4 nanocomposite, b) SA/ADH/Fe_3O_4 nano-composite. （target DNA: 10^{-6} M）

Construction of the SPE aptasensor

As shown in Fig. 4A, the SPE aptasensor (16 copies/pic) was successfully constructed. Meanwhile, kits with switches were also made. These provided a relatively sealed space, required less reagent (40～200 μL), and avoided external interference in the detection. The reproducibility of the SPE aptasensor was evaluated by detecting the same target DNAs using 10 SPE aptasensors in the same conditions. A relative standard deviation (RSD) of 6.4 % was obtained (Fig. 4B-a). Moreover, a RSD of 4.6 % was obtained for 10 measurements of the SPE aptasensor (Fig. 4B-b). Both values indicate the good reproducibility of the SPE aptasensor.

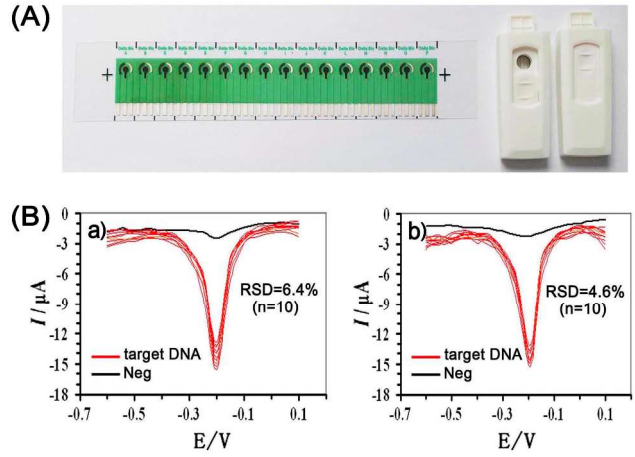

Fig. 4. Construction of SPE aptasensor. (A) SPE aptasensor and a kit with switch. (B) Reproducibility of SPE aptasensor. a) same target DNA using 10 SPE aptasensors; b) a SPE aptasensor for 10 measurements. （target DNA: 10^{-6} M）

Calibration curve of the SPE aptasensor

Under the optimised experimental conditions, the SPE aptasensor was incubated with a series of target DNA (10^{-14}～10^{-4} M), and the corresponding DPVs were recorded. As shown in Fig. 5A, the DPV current response was quite flat in 10^{-14}～10^{-12} M (defined as S/N=3), indicating that the lowest detection limit was 10^{-12} M, and the highest detection limit was approximately 10^{-6} M. The hemin/G-quadruplex is a widely used electrochemical material in signal amplification. It had been reported that the electric signal increases logarithmically with the targeted DNA concentration.[29] In this work, the electrochemical signal increased linearly with the logarithm of target DNA concentration too, with a linear range from 10^{-12} to 10^{-6} M. The linear equation was y=2.896 logC+37.8 (R^2=0.9899) (Fig. 5B). The results imply that the employment of SA/ADH/Fe_3O_4 nanocomposites yielded a great improvement in catalytic ability of the ADH and hemin/G-quadruplex acted as a NADH oxidase and a HRP-mimicking DNAzyme.

An electrochemiluminescence (ECL) strategy with rolling circle amplification (RCA) was previously reported by our lab.[2] Compared with the previous research, this SPE strategy is not advantageous in terms of sensitivity. The main reason is because ECL has higher sensitivity (10^{-15}M), and the DNA was amplified by RCA in the ECL strategy. However, in terms of sensor miniaturisation and application in point of care testing (POCT), this SPE strategy has more advantages.

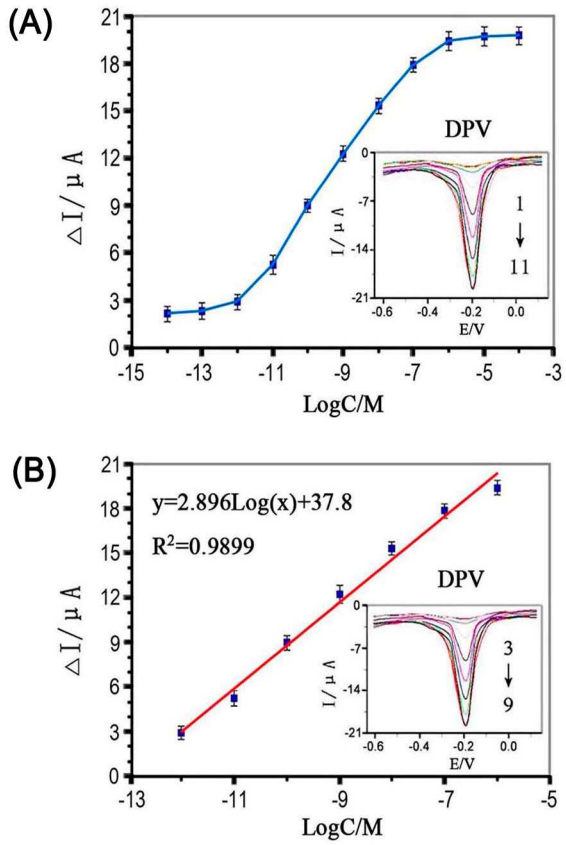

Fig. 5. Calibration curve of the SPE aptasensor. (A) DPVs of SPE aptasensor with target DNA. (B) DPVs and calibration curve of SPE aptasensor with target DNA. (1～11: 10^{-14} ～10^{-4} M target DNA)

Specificity and stability of the SPE aptasensor

To investigate the specificity of the SPE aptasensor, eight wound infection associated bacteria, [30-32] *C. perfringens*，*C. tetani, S. aureus*, *E. coli, P. aeruginosa, S. epidermidis, S. pneumoniae, B. acinetobacter,* and a synthesised target DNA were detected. As shown in Fig. 6A, the DPV responses to eight wound infection associated bacteria were close to that of the negative sample. In contrast, there were significant electrochemical signals from the synthesised target DNA and *C. perfringens*. The results indicated that the SPE aptasensor had excellent specificity for *C. perfringens* detection. Additionally, we demonstrated the stability of the SPE aptasensor using a long-term storage assay (Fig 6B). The electrochemical signal retained 90.5% of its initial current after 20 days of storage at 4°C, indicating that its stability is sufficient for use in *C. perfringens* detection.

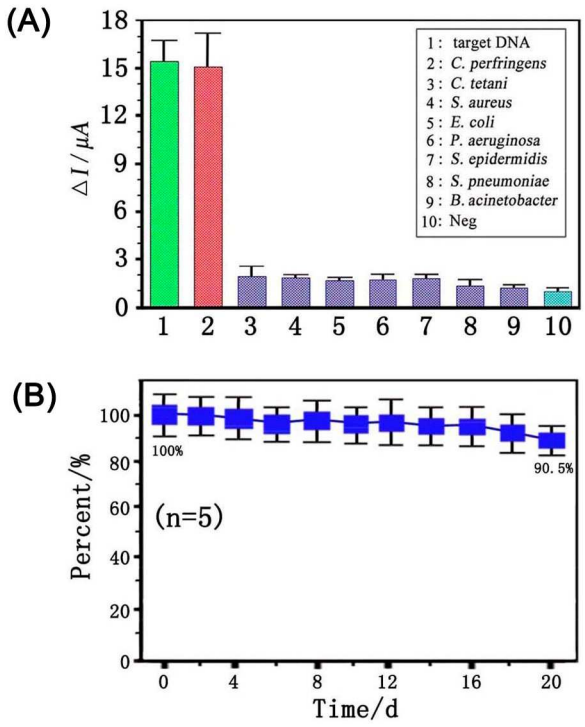

Fig. 6. Specificity and stability of the SPE aptasensor (ip of DPVs). (A) Specificity of the SPE aptasensor; (B) Stability of the SPE aptasensor. (DNAs: all in 10^{-6} M)

Application of the SPE and comparison with PCR

To assess the reliability of the SPE aptasensor for *C. perfringens* detection, the practical applicability of the SPE was investigated by adding different concentrations of *C. perfringens* into 10-fold-diluted human real wound secretion samples obtained from the Xinqiao Hospital (Chongqing, China), which were then detected by SPE aptasensor and PCR at the same time. As shown in Fig. 7A, B, *C. perfringens* was detected by both methods. The results demonstrated the excellent promise for the detection of *C. perfringens* in real biological samples. Furthermore, there were no significant differences in recovery (Fig. 7C) and regression of concentration between SPE aptasensor and PCR (Fig. 7D). Thus, this SPE strategy has a high accuracy compared with PCR and can be applied preliminarily to clinical samples.

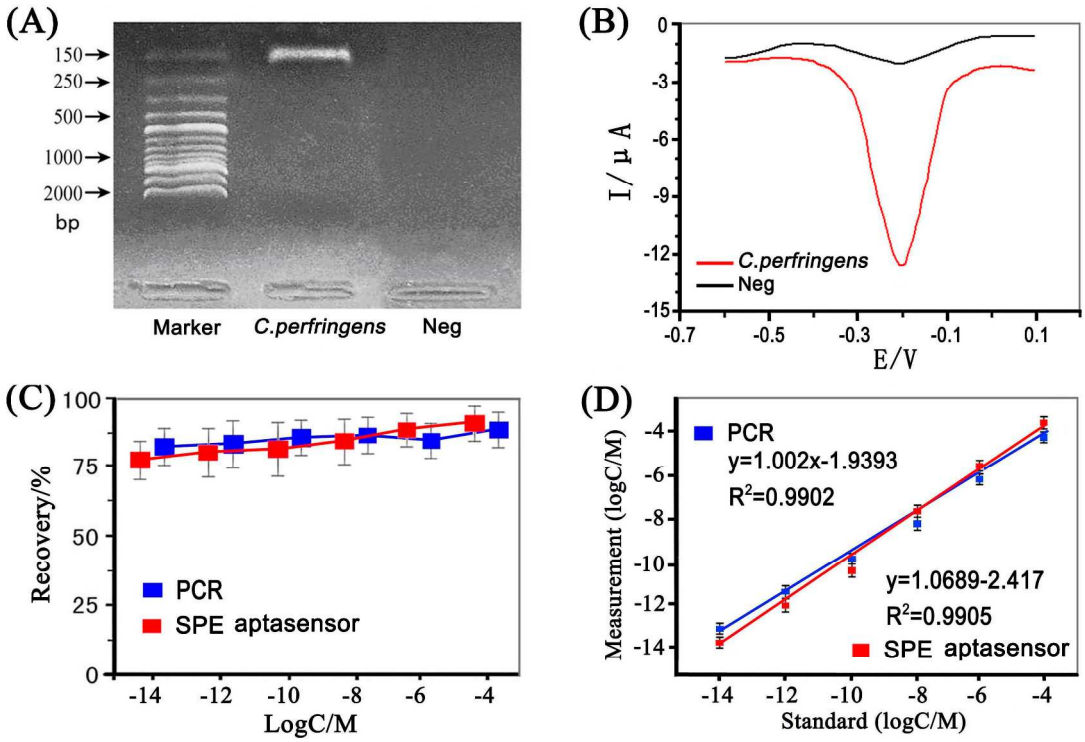

Fig. 7. Application of the SPE aptasensor and comparison with PCR. (A) Electrophoresis of PCR product in 2% agarose gel. (B) DPV curves of SPE measurements. (C) Comparsion of recovery between SPE aptasensor and PCR. (D) Comparsion of regression between SPE aptasensor and PCR. (standard: 10^{-14}～10^{-4}M target DNA)

Conclusions

C. perfringens is difficult to culture and as such, often escapes detection. In this study, a SPE strategy based on MB/AuNPs/graphene/GCE and SA/ADH/Fe_3O_4 nanocomposite was successfully constructed. The use of AuNPs/graphene/GCE enlarged the surface area and enhanced the immobilisation of the capture probe (MB). The combination of the SA/ADH/Fe_3O_4 nanocomposite with the hemin/G-quadruplex enabled the progressive amplification of the electrochemical signal. The results showed a high sensitivity of 10^{-12} M and a wide linear range from 10^{-12} to 10^{-6} M. Compared with PCR, there were no significant differences in recovery and regression of concentration, suggesting that this method has high accuracy. Thus, this SPE strategy may be a promising alternative to detect *C. perfringens* without bacterial culture and DNA amplification in POCT.

Conflict of interest

We have no conflicts of interest to declare related to the submission of this article.

Acknowledgements

This work received the support of the National Natural Science Foundation of China (NSFC: 81371898). We appreciate the valuable comments from other members of our laboratories.

References

1. N. J. Shih and R. G. Labbe, *Appl Environ Microbiol*, 1996, **62**, 1441-1443.
2. D. N. Jiang, F. Liu, C. Liu, L. L. Liu, Y. Li and X. Y. Pu, *Anal Methods-Uk*, 2014, **6**, 1558-1562.
3. S. Singh, K. Angra, B. Davis and B. Shokrani, *Case Rep Obstet Gynecol*, 2014, **2014**, 282141.
4. S. B. Wu, N. Rodgers and M. Choct, *Appl Environ Microbiol*, 2011, **77**, 1135-1139.
5. D. K. O'Brien and S. B. Melville, *Infect Immun*, 2004, **72**, 5204-5215.
6. E. Borrmann, F. Schulze, K. Cussler, I. Hanel and R. Diller, *Vet Microbiol*, 2006, **114**, 41-50.
7. V. Leflon-Guibout, J. L. Pons, B. Heym and M. H. Nicolas-Chanoine, *Anaerobe*, 1997, **3**, 245-250.
8. S. F. Al-Khaldi, D. Villanueva and V. Chizhikov, *Int J Food Microbiol*, 2004, **91**, 289-296.
9. A. Povazan, A. Vukelic, T. Savkovic and T. Kurucin, *Bosn J Basic Med Sci*, 2012, **12**, 33-36.
10. Y. Hitsumoto, N. Morita, R. Yamazoe, M. Tagomori, T. Yamasaki and S. Katayama, *Anaerobe*, 2014, **25**, 67-71.
11. W. Guan, X. Duan and M. A. Reed, *Biosens Bioelectron*, 2014, **51**, 225-231.
12. M. Rana, M. Balcioglu, N. Robertson and M. V. Yigit, *Analyst*, 2014, **139**, 714-720.
13. N. Kaneko, K. Horii, S. Kato, J. Akitomi and I. Waga, *Anal Chem*, 2013, **85**, 5430-5435.
14. X. Meng, Y. Zhou, Q. Liang, X. Qu, Q. Yang, H. Yin and S. Ai, *Analyst*, 2013, **138**, 3409-3415.

15. P. Jing, W. Xu, H. Yi, Y. Wu, L. Bai and R. Yuan, *Analyst*, 2014, **139**, 1756-1761.
16. V. Sosa, N. Serrano, C. Arino, J. M. Diaz-Cruz and M. Esteban, *Talanta*, 2014, **119**, 348-352.
17. Y. Li, L. Deng, C. Deng, Z. Nie, M. Yang and S. Si, *Talanta*, 2012, **99**, 637-642.
18. S. Mu, X. Wang, Y. T. Li, Y. Wang, D. W. Li and Y. T. Long, *Analyst*, 2012, **137**, 3220-3223.
19. M. Pandiaraj, N. K. Sethy, K. Bhargava, V. Kameswararao and C. Karunakaran, *Biosens Bioelectron*, 2014, **54**, 115-121.
20. Z. Cai, Y. Song, Y. Wu, Z. Zhu, C. J. Yang and X. Chen, *Biosens Bioelectron*, 2013, **41**, 783-788.
21. E. Golub, R. Freeman and I. Willner, *Anal Chem*, 2013, **85**, 12126-12133.
22. N. Wen, W. Liu, Y. Hou and Z. Zhao, *Appl Biochem Biotechnol*, 2013, **170**, 370-380.
23. N. A. Zubir, C. Yacou, J. Motuzas, X. Zhang and J. C. Diniz da Costa, *Sci Rep*, 2014, **4**, 4594.
24. E. Golub, R. Freeman and I. Willner, *Angew Chem Int Edit*, 2011, **50**, 11710-11714.
25. F. Valentini, E. Ciambella, V. Conte, L. Sabatini, N. Ditaranto, F. Cataldo, G. Palleschi, M. Bonchio, F. Giacalone, Z. Syrgiannis and M. Prato, *Biosens Bioelectron*, 2014, **59**, 94-98.
26. A. F. Maheux, E. Berube, D. K. Boudreau, R. Villeger, P. Cantin, M. Boissinot, L. Bissonnette and M. G. Bergeron, *Appl Environ Microbiol*, 2013, **79**, 7654-7661.
27. A. Lovland, M. Kaldhusdal and L. J. Reitan, *Avian Pathol*, 2003, **32**, 527-534.
28. M. M. Silva, A. C. Dias, M. T. Cordeiro, E. Marques, Jr., M. O. Goulart and R. F. Dutra, *Talanta*, 2014, **128**, 505-510.
29. Y. Yuan, M. Gao, G. Liu, Y. Chai, S. Wei and R. Yuan, *Anal Chim Acta*, 2014, **811**, 23-28.
30. P. V. Gawande, K. P. Leung and S. Madhyastha, *Curr Microbiol*, 2014, **68**, 635-641.
31. O. A. Aiyegoro, A. J. Afolayan and A. I. Okoh, *Biol Res*, 2009, **42**, 327-338.
32. A. M. Parr, D. E. Zoutman and J. S. Davidson, *Ann Plast Surg*, 1999, **43**, 239-245.

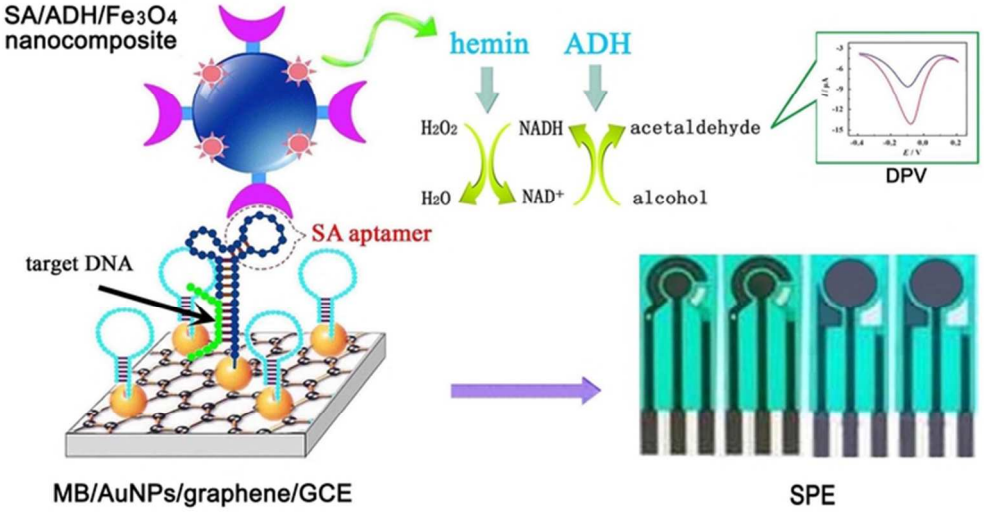

An electrochemical strategy based on molecular beacon, hemin/G-quadruplex, and SA/ADH/Fe3O4 nanocomposites.
61x32mm (300 x 300 DPI)